

**MINISTRY OF EDUCATION
AND TRAINING**

**VIETNAMESE ACADEMY OF
SCIENCE AND TECHNOLOGY**

GRADUATE UNIVERSITY OF SCIENCE AND TECHNOLOGY



Nguyen Thi Thu Hoa

**SYNTHESIS AND INVESTIGATION OF THE
ELECTROCHEMICAL CHARACTERISTICS OF Co, F
DOPPED AND CO-DOPPED (Na,Li)MnO₂ OXIDE AS THE
CATHODE FOR SODIUM-ION BATTERIES**

SUMMARY OF DISSERTATION ON MATERIALS SCIENCE

Major: Electronic material

Code: 9 44 01 23

Ha Noi - 2026

The dissertation is completed at: Graduate University of Science and Technology, Vietnam Academy Science and Technology

Supervisors:

1. Supervisor 1: Assoc. Prof. Dr. Nguyen Van Nghia, Hanoi Architectural University.
2. Supervisor 2: Prof. Dr. Vu Dinh Lam, Graduate University of Science and Technology, Vietnam Academy of Science and Technology.

Referee 1:

Referee 2:

The dissertation is defended before the Doctoral Dissertation Evaluation Council at the Graduate University of Science and Technology, Vietnam Academy of Science and Technology at

The dissertation can be found at:

1. Graduate University of Science and Technology Library
2. National Library of Vietnam

INTRODUCTION

1. The urgency of the dissertation

Today, most mobile devices such as laptops, mobile phones, robots, electric cars and motorcycles, medical equipment, solar energy conversion systems, etc., require energy storage devices. Therefore, energy storage sources are becoming an urgent requirement in the present and future. Research on energy storage devices has being focused on by many scientists and technology companies in various fields.

Lithium-ion batteries (LIBs) were commercialized in 1991 and remained as the most popular energy storage component to date, but Lithium (Li) reserves on Earth are limited. Therefore, it is necessary to find alternative storage devices to LIBs in the future. Many storage devices have been researched to replace LIBs, such as potassium ion batteries, magnesium ion batteries, sodium ion batteries (SIBs), etc. Among these, SIBs are receiving the most attention because they have a similar operating principle to LIBs and the sodium source is abundant. However, SIBs also have limitations such as cycling ability and rate capability. To overcome the limitations, scientists are working to find materials which have good electrochemical properties to serve as the positive electrode for the SIB.

The materials used for the positive electrode of SIBs can classified into four main groups: layered transition metal oxides; polyionic materials; Russian blue and organic compounds. Among them, manganese-based transition metal oxides (Na_xMnO_2) are the most promising due to their high operating potential, superior theoretical capacity, and simple synthesized process. However, Na_xMnO_2 materials have limitations such as insufficient specific capacity to compete with current LIBs and rapid capacity loss during cycling. Many studies have shown that partial replacing Na^+ ions by Li^+ ions

in the Na_xMnO_2 crystal to form the system $(\text{Na},\text{Li})\text{MnO}_2$ can help stabilize the layered structure, limit the sliding of the MnO_2 layers, and thus improve the cycling performance of the material. Therefore, instead of pure Na_xMnO_2 , many studies have been conducted on the $(\text{Na},\text{Li})\text{MnO}_2$ materials.

Arising from practical needs, the dissertation "Synthesis and investigation of the electrochemical characteristics of Co, F doped and co-doped $(\text{Na},\text{Li})\text{MnO}_2$ oxide as the cathode for sodium-ion batteries" was chosen.

2. The objectives of the dissertation

Synthesized Co, F doped and co-doped $(\text{Na},\text{Li})\text{MnO}_2$ oxides, which have a hexagonal structure, P63/mmc space group, and particle size $< 5\mu\text{m}$ suitable for cathodes in SIBs. Simultaneously, to clarify the influence of doping elements on the structure and electrochemical properties of materials.

3. Content of the Research

- Study to synthesize Co, F doping and co-doping $(\text{Na},\text{Li})\text{MnO}_2$ oxide by solid-state reaction method and sol-gel method.
- Investigating the structural and morphological characteristics of materials.
- Fabrication SIB with cathode made from synthesized material.
- The electrochemical properties of the synthesized materials were studied to analyze the influence of doping elements on the electrochemical properties of the $(\text{Na},\text{Li})\text{MnO}_2$ oxide.

4. Scientific and Practical Implications

This dissertation has contributed to provide more knowledge on layered oxide materials with high electrochemical properties used as cathodes for SIBs, a research direction that is receiving great attention from the scientific community worldwide. Through the systematic study of Co,

F doped and co-doped oxide material synthesized by solid-state reaction and sol-gel methods, the dissertation has clarified the role of each doping element in influencing the structure and electrochemical properties of the materials. The research results show that: both a and c lattice constants of Co doped (Na,Li)MnO₂ material synthesized by solid-state reaction method were decreased, reflecting a relatively uniform contraction of the crystalline structural framework. However, the Co doped and (Co, F) co-doped (Na,Li)MnO₂ by the sol-gel method, the a lattice constant was decreased but the c constant was increased, indicating that the MO₂ framework in the layer plane contracted but the spacing between MO₂ layers was expanded. These structural changes directly affect the electrochemical properties of the material. The decrease of the a constant makes the MO₂ sheet more stable, contributing to improve structural stability and thus improving the material's cycle performance. Meanwhile, the increase in the c constant reflects the expansion of the spacing between MO₂ layers, allowing Na⁺ ions to easily insert into/out and diffuse inside the bulk structure of the material, thereby improving the material's specific capacity.

In addition, Co can directly participate in the charge exchange process during cycling, contributing to increase capacity of the material. Co also increases the electrical conductivity of the electrode, improving the kinetics of the electrochemical reaction. Meanwhile, anion F⁻ replaced O²⁻ lead to an increase of the number of electrochemically active sites in the crystal lattice, thereby improving the material's specific capacity.

In practical terms, this dissertation has contributed to guiding the development of electrode materials with high electrochemical properties for SIBs from common, low-cost, and environmentally friendly raw materials, thereby reducing dependence on rare and expensive metals. The dissertation can be a

valuable reference for scientists, researchers, and graduate students studying the field of positive electrodes for SIBs.

5. Novel Contributions

1) The dissertation successfully fabricated Co, F doped and co-doped into (Na,Li)MnO₂ oxide, which has hexagonal structure with P63mmc space groups and particle sizes < 5μm suitable for use as cathodes for SIBs: (1) Na_{0.67}Li_{0.33}Mn_{0.95}Co_{0.05}O₂ (NLMC) material provides discharge specific capacity of 111.89 mAh.g⁻¹ at a current density of 11 mA g⁻¹ and 63 mAh g⁻¹ at high current density 110 mA g⁻¹. Cycle efficiency is about 97.9% (after 100 cycles at a current density of 1 mA g⁻¹); (2) The Na_{0.8}Li_{0.1}Mn_{0.8}Co_{0.1}O₂ (Co-NLM) material provides a discharge specific capacity of 121.44 mAh g⁻¹ at 8 mA g⁻¹ and 90.25 mAh g⁻¹ at 100 mA g⁻¹. Cycle efficiency: 92.11% (after 100 cycles at 8 mA g⁻¹); (3) Na_{0.8}Li_{0.1}Mn_{0.8}Co_{0.1}F_{0.1}O₂ (CoF-NLM) material provides a specific capacity of 135 mAh g⁻¹ at a current density of 8 mA g⁻¹ and 101.15 mAh g⁻¹ at a high current density of 100 mA g⁻¹. Cycle efficiency: 94% (after 100 cycles at a current density of 8 mA g⁻¹).

2) The dissertation has demonstrated that Co, F doping and co-doping (Na,Li)MnO₂ affect the structure and electrochemical properties of non doping material. Specifically: (i) Co doping synthesized by solid-state reaction method simultaneously reduces both *a* and *c* lattice parameters. While Co, F doping and co-doping (Na,Li)MnO₂ synthesized by sol-gel method reduces *a* lattice constant and increases *c* lattice constant. At the same time, the dissertation has also demonstrated that changes in lattice parameters affect the electrochemical properties of the material in different aspects; (ii) The dissertation has clarified the influence of each dopant on the electrochemical properties of (Na,Li)MnO₂ oxide material: Co²⁺ directly participates in redox reactions to contribute to the specific capacity of the material. At the same time, Co increases electrical conductivity, helping to improve the kinetics of the electrochemical reaction

occurring at the electrode; F increases the activity of transition metal ions, contributing to the increased capacity of the material.

Dissertation structure: The dissertation comprises 141 pages, including an Introduction, 4 content chapters, and the Conclusions.

CHAPTER 1. OVERVIEW OF THE STUDY

1.1. Overview of Sodium Ion Battery Systems

1.1.1. History of the formation and development of sodium ion batteries

Starting in the late 1970s, SIB systems were studied alongside LIB systems, but due to SIB's significantly inferior electrochemical characteristics compared to LIB, SIB received less attention, leading to LIB commercialization in 1991. However, the recent boom in electric vehicles and energy storage using LIB could lead to a lithium shortage. Therefore, more attention is being paid to the development of SIBs.

From 2015 to 2018, research on SIBs experienced a boom in both the number of scientific publications and industrial investment. Since 2018, research on SIBs has entered a new phase, shifting from the exploration of basic materials to efforts aimed at optimizing the entire battery system, increasing energy density, and most importantly, bringing the technology to market. As of 2025, many SIB (Small Electric Battery) variants have been installed in small electric vehicles in China. It is predicted that SIB will be the leading technology in the low-cost, moderately energy-dense, and highly safe battery segment in the future.

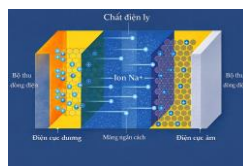


Figure 1.1. Operating principle of SIB.

1.1.2. Structure of a Sodium Ion Battery

SIB consists of four main parts: the positive electrode, the negative electrode, the membrane separating the two electrodes, and the electrolyte.

1.1.3. Energy storage mechanism of sodium ion batteries

During the charging process, electrical energy causes the movement of electrons from the cathode to the anode through the external circuit. At the cathode, an oxidation reaction takes place, producing Na^+ ions. These Na^+ ions move from the cathode to the anode, and then insert into the anode material. At the anode, a reduction reaction then takes place.

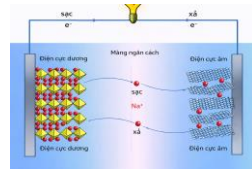


Figure 1.2. Operating principle of SIB

During discharge, Na^+ ions move from the anode to the cathode and fill the cathode material, where a reduction reaction occurs. To balance the charge, when a Na^+ ion moves from the anode to the cathode in the battery, in the external circuit, one electron moves from the anode to the cathode through the load resistor, meaning a current flows from the positive to the negative electrode.

1.1.4. Factors affecting the storage capacity of sodium ion batteries

The energy storage capacity of SIBs is evaluated through the following parameters: (i) Specific capacity; (ii) Energy density; (iii) Cycle efficiency; (iv) Coulomb efficiency. These parameters are influenced by key factors including: (1) cathode material, (2) Electrode, (3) Electrode fabrication parameters and operating conditions, (4) Anode material. Among these factors, the cathode is the most important, as it is the "source" of Na^+ ions for the system and is also one of the main causes of cycling capacity degradation.

1.2. Overview of positive electrode materials for sodium ion batteries

Main groups of materials that have been studied as cathodes for SIBs include: layered transition metal oxide; Polyionic material; Russian blue material; and organic compounds. Each type of materials has its own advantages and limitations. Among them, layered transition metal oxide are receiving the most attention due to their simple structure, ease of synthesis, and potential for high theoretical capacity and operating voltage .

1.3. Layered structure Na_xMO_2 oxide.

1.3.1. Na^+ ion storage mechanism of Na_xMO_2 material

In O3 material ($x \geq 1$), adjacent empty positions allow Na^+ ions to move. Movement is almost nonexistent. When moving, Na^+ ions follows a "zig-zag" path from the octahedral position to the tetrahedral void. As a result, the O3 material has slow diffusion kinetics, poor charge-discharge rates, and its structure is significantly altered during the electrochemical operation of the battery.

In P2 type materials ($x = 0.5-0.83$), there are many Na^+ ion vacancies, creating pathways for Na^+ ions to easily move directly from one prismatic position to another. Therefore, P2 type materials have faster Na^+ ion diffusion kinetics, better charge-discharge rates, and a more stable structure than O3 type materials.

1.3.2. Cation oxidation-reduction mechanism in Na_xMO_2 material

When SIB is operating, Na^+ ions continuously insert into and exit the cathode material. To balance the charge in the electrode, the transition metals in the crystal lattice participate in redox reactions to produce Na^+ ions. For the system, the cation redox mechanism has high stability and good reversibility. However, this mechanism is limited by the number of electrons the transition metal exchanges in each redox reaction, which is limited .

1.3.3. Anion oxidation-reduction mechanism in Na_xMO_2 material

When SIBs are in operation, cation redox mechanisms are the primary contributors to the material's capacity and operating potential. However, oxygen within the crystal lattice can also directly participate in redox activity. This reaction can occur in parallel with cation redox reactions to generate additional capacity. However, this process often causes irreversible phase transitions, loss of network oxygen, and reduce material cycle performance.

1.4. Layered manganese oxide materials

1.4.1. Advantages of manganese-based layered oxide materials:

(1) Source abundant raw materials, cheap, and less toxic; (2) Mn has a rich valence; (3) Materials have diverse crystal structures; (4) The main redox reaction of the material occurs at a voltage level where both the positive electrode and the electrolyte operate stably .

1.4.2. Disadvantages of manganese-based layer oxides: phase transition irreversible, Jahn-Teller effect, interface degradation, poor air stability, leading to rapid cycling capacity degradation.

1.4.3. Measures to overcome the disadvantages of manganese-based layered oxides:

To overcome the disadvantages of layered Mn oxide materials, many different techniques have been proposed and applied such as: (1) Synthesis of integrated phase materials; (2) Control of particle morphology and structure; (3) Replacement chemical elements; (4) Surface coating. In which, replacing chemical elements is a simple and highly effective method.

To somewhat limit the variation of the crystal structure, instead of pure Na_xMnO_2 , many studies have been conducted on oxide-based $(\text{Na},\text{Li})\text{MnO}_2$ material systems.

1.5. Research in Vietnam

In recent years, several domestic research groups have begun to show interest in cathode materials for sodium ion batteries, mainly focusing

on layered transition metal oxides such as Mn, Ni, Co, and Fe. These materials are synthesized using sol-gel or solid-state reaction methods and yield specific capacities in the range of 100–170 mAh g⁻¹. However, many material systems still face limitations in structural stability and capacity degradation during the cycling process. Therefore, research on layered oxide materials based on the (Na,Li)MnO₂ system with doping strategies to improve capacity and cycle stability is a necessary. Based on this review, the dissertation focuses on studying Co, F doped and co-doped (Na,Li)MnO₂ materials as the cathode for sodium ion batteries.

1.6. Conclusion of Chapter 1

Chapter 1 presented the following issues: (1) LIB is a popular storage device on the market, but lithium resources are limited, so a replacement for LIB needs to be found in the future. SIB is a potential replacement for LIB. However, SIB has limited energy density and cycle efficiency. To overcome this limitation, research is needed to optimize the cathode material because the cathode is a key factor determining the success of SIB; (2) Layered transition metal oxides, especially layered Mn-based oxides, are widely studied because It has many outstanding advantages. However, this material has a rapidly decreasing capacity over time. To overcome this drawback, Li⁺ ions introduced into the structure to form the (Na,Li)MnO₂ oxide system is considered as an effective approach to stabilize the crystal framework and contribute to improving the reversibility of the electrochemical reaction occurring on the electrode; (3) Doping other chemical elements such as Ni, Co, F,... into (Na,Li)MnO₂ oxide material have been shown to be effective measures to improve the electrochemical properties of this material.

CHAPTER 2. RESEARCH METHODS

2.1. Cathode material synthesized methods for SIB

2.1.1. Synthesis Co doped (Na,Li)MnO₂ oxide by solid-state reaction method

The Na_{0.67}Li_{0.33}MnO₂ (NLM) and Na_{0.67}Li_{0.33}Mn_{0.95}Co_{0.05}O₂ (NLMC) materials were synthesized by solid-state reaction method (Figure 2.1).

Table 2.1. Sample designations and precursor quantities.

No.	Symbol	Na ₂ CO ₃	Li ₂ CO ₃	MnCO ₃	CoCO ₃
1	NLM	1.166 (g)	0.406 (g)	3.449 (g)	0.0 (g)
2	NLMC	1.166 (g)	0.406 (g)	3.276 (g)	0.178 (g)

2.1.2. Synthesis Co, F doped and co-doped (Na,Li)MnO₂ oxide by sol-gel method

The Na_{0.8}Li_{0.1}Mn_{0.9}O₂ (NLM), Na_{0.8}Li_{0.1}Mn_{0.8}Co_{0.1}O₂ (NLMC), Na_{0.8}Li_{0.1}Mn_{0.8}F_{0.1}O₂ (F-NLM) materials and Na_{0.8}Li_{0.1}Mn_{0.8}Co_{0.1}F_{0.1}O₂ (CoF-NLM) were synthesized by the sol-gel method (Figure 2.2).

Table 4.1. Sample designations and precursor quantities.

Symbol	Na ₂ CO ₃ (g)	Li ₂ CO ₃ (g)	LiF (g)	Mn(CH ₃ COO) ₂ ·4H ₂ O (g)	Co(CH ₃ COO) ₂ ·4H ₂ O (g)	C ₂ H ₄ O ₂ ·H ₂ O (g)
NLM	1.780	0.155	0	8.823	0	7.985
NLMC	1.780	0.155	0	7.843	0.996	7.985
F-NLM	1.780	0.155	0	8.823	0	7.985
CoF-NLM	1.780	0	0.104	7.843	0.996	7.985

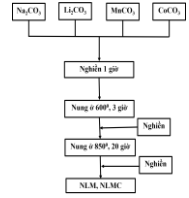


Figure 2.1. Material fabrication process

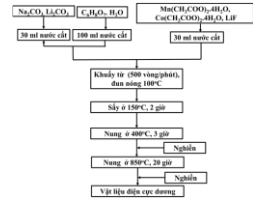


Figure 2.2. Material fabrication process

2.2. Fabrication of sodium ion batteries

2.2.1. Fabrication of transition metal oxide cathode

The cathode material was mixed with carbon black and PVDF in a mass ratio of 8:1:1, then dispersed in NMP solvent. This mixture forms a smooth, viscous slurry. This slurry is spread onto a thin aluminum foil 15 μm thick and dried at 100 °C under vacuum for 12 hours to obtain a sheet of cathode. The cathode is pressed using a roller press and cut into circular cathode electrodes.

2.2.2. Assembling the sodium ion battery

The battery assembly process is carried out in a Glovebox. Cathode, anode, the separate membrane is arranged carefully inside a standard CR 2032 battery casing. Then, added 0.3-0.5 ml of electrolyte solution. Finally, everything is pressed on a hydraulic press to obtain the complete SIB.

2.3. The methods for study the structure and morphology of cathode materials

2.3.1. X-ray Diffraction (XRD)

This dissertation uses X-ray diffraction (XRD) to determine the structure of the material, and the values of the lattice constants.

2.3.2. Scanning electron microscopy (SEM) and energy dispersive X-ray/ spectroscopy (EDX/EDS-mapping)

SEM is used to determine the morphology of material surface, EDX/EDS-mapping to determine the elemental composition and distribution of elements in the material.

2.3.3. Transmission Electron Microscopy (TEM)

TEM is used to determine morphology inside of the material.

2.3.4. Inductively coupled plasma mass spectrometry (ICP-MS)

ICP-MS is used to determine the content of elements in materials.

2.3.5. X-ray Photoelectron Spectroscopy (XPS)

XPS is used to determine the composition and valence state of elements on the surface of the material compounds.

2.4. The methods for study the electrochemical properties of materials

2.4.1. Cyclic Voltammetry (CV)

Circular voltage (CV) scanning is used to analyze oxidation processes. Redox reactions occur within the electrode material.

2.4.2. Galvanostatic Charge–Discharge (GCD)

GCD is used to determine parameters such as specific capacity and rate capability, cycle efficiency. From that, the quality of the electrode material can be evaluated.

2.4.3. Electrochemical Impedance Spectroscopy (EIS)

Electrochemical impedance spectroscopy (EIS) is used to analyze the diffusion dynamics of Na^+ ions, determine electrical conductivity, ionic conductivity, etc. From there, the electrical conductivity and performance of the electrode can be evaluated.

2.5. Conclusion of Chapter 2

Chapter 2 presented the synthesis and research methods used in this dissertation: (1) Co, F doped and co-doped $(\text{Na,Li})\text{MnO}_2$ synthesized method (solid-state reaction method, sol-gel method); (2) Fabricating a complete CR2032 battery method; (3) Investigating morphology, structure, and composition methods (XRD, SEM, TEM, EDX, ICP-MS); (4) Studying the electrochemical properties of the material methods (GCD, CV, EIS).

CHAPTER 3. INFLUENCE OF Co DOPPING ON THE STRUCTURE AND ELECTROCHEMICAL PROPERTIES OF $(\text{Na,Li})\text{MnO}_2$ OXIDE

3.1. The structure and morphology of NLM and NLMC materials

3.1.1. The phase structure results of NLM and NLMC materials

The XRD patterns of NLM and NLMC are similar. The main diffraction peaks matches the JCPDS standard spectrum No. 27-0751, indicating that the materials have a P2 hexagonal structure, belonging to the $\text{P6}_3/\text{mmc}$ space group. In addition, there are 2 weak diffraction peaks corresponding to the crystal lattice planes (003) and (104) of Li_2MnO_3 .

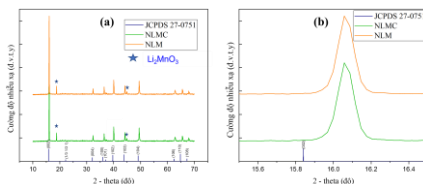


Figure 3.1. (a) X-ray diffraction pattern and (b) peak magnification region (002) of the materials.

The magnified region of peak (002) shows diffraction peaks shifted toward a larger 2θ angle, indicating that the lattice plane spacing has slightly decreased.

3.1.2. The elemental composition determination results in synthesized materials

EDX analysis results revealed the presence of Na, Mn, and O elements in NLM and Na, Mn, Co, and O elements in NLMC material. The approximate ratio of atoms in a material is determined by ICP-MS technique. The results obtained are consistent with the atomic ratios in the original salt mixture.

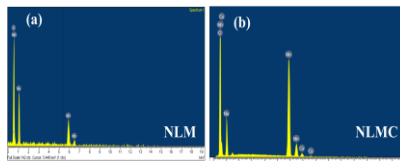


Figure 3.2. EDX results of NLM and NLMC

3.1.3. The morphology of synthesized materials

SEM images of the materials show that both materials have polyhedral shapes with sizes ranging from 1 to 3 μm and stick together (Figure 3.3).

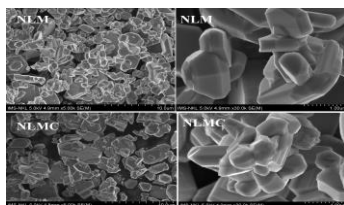


Figure 3.3. SEM images of NLM and NLMC

3.2. The electrochemical properties of synthesized materials

3.2.1. Galvanostatic Charge–Discharge results

In figure 3.4, the NLMC material has a specific discharge capacity at the second cycle of $111.89 \text{ mAh g}^{-1}$, this result is higher compared to the NLM material (86 mAh g^{-1}) and also a considerable improvement over some previously published materials.

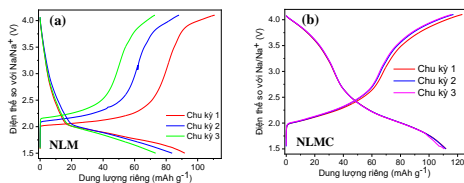


Figure 3.4. Charging and discharging paths for the first 3 cycles of NLM and NLMC.

Both NLM and NLMC materials exhibit a decrease in specific capacity as current density increases (Figure 3.6). At a high current density of 110 mA g^{-1} , the discharge specific capacity of the NLMC material remained at 63 mAhg^{-1} , while those of the NLM material was only about 17 mAh g^{-1} . This result demonstrated that the NLMC material has a better charging and discharging rate.

Figure 3.7 shows that, after 100 cycles, the discharge specific capacity of the NLMC material at a current density of 11 mAhg^{-1} still maintains 97.9% of the discharge capacity of the second cycle. This value represents a significant improvement over many other NLM materials (88.6% after 30 cycles) and also a considerable improvement over previously published materials.

3.2.2. Cyclic Voltammetry results

On the CV curve (Figure 3.8), there are three pairs of redox peaks. The pair at $2.24 \text{ V}/1.61 \text{ V}$ is assigned to the redox reaction of the $\text{Mn}^{+4}/\text{Mn}^{+3}$ pair. The second pair at $3.10 \text{ V}/3.01 \text{ V}$ is assigned to the redox reaction of the $\text{Co}^{2+}/\text{Co}^{3+}$ pair. The exact origin of the third pair at

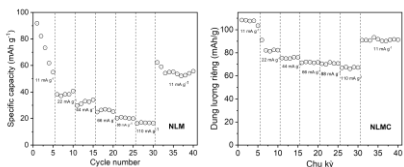


Figure 3.6. The charging and discharging speeds result of NLM and NLMC.

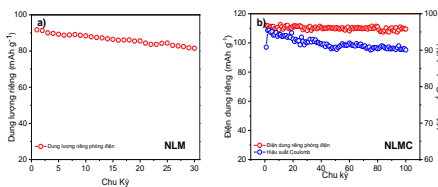


Figure 3.7. Cycle performance of materials.

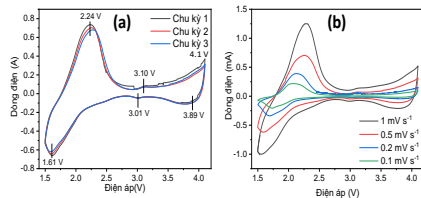


Figure 3.8. (a) CV curve of NLMC at 0.1 mVs^{-1} and at different scan rates.

4.1 V/3.89 V is unknown. The results demonstrate that Co directly participated in the charge exchange process to create the capacity of the material.

The sodium ion diffusion coefficient is calculated from the Randles–Sevcik equation:

$$I_p = 2.69 \times 10^{-5} \times n^{3/2} \times A \times D^{1/2} \times C \times v^{1/2}$$

As a result, the sodium ion diffusion coefficient of NLMC larger than the diffusion coefficient of some other materials, which has been previously published. Therefore, NLMC materials exhibit good electrochemical properties.

3.2.3. The electrochemical impedance spectrum analysis result

Figure 3.10 shows the EIS graphs of the two materials in the frequency range from 1 to 10^5 Hz. The equivalent circuit and the values of the elements in the equivalent circuit were analyzed using Nova 1.11 software. As a result, the R_s , R_F , and R_{ct} values of the NLMC material are 2.97, 0.45, and 44.52 Ω , respectively. These values are lower than those of NLM and $\text{NaLi}_{0.2}\text{Mn}_{0.6}\text{Ni}_{0.2}\text{O}_2$, $\text{Na}_{1.0}\text{Li}_{0.2}\text{Mn}_{0.7}\text{Ti}_{0.1}\text{O}_2$.

The electrochemical characteristics of NLMC have confirmed that the electrochemical properties of NLMC have been significantly improved compared to NLM materials. The specific capacity of NLMC

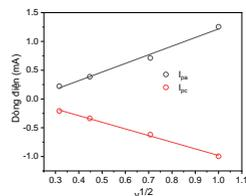
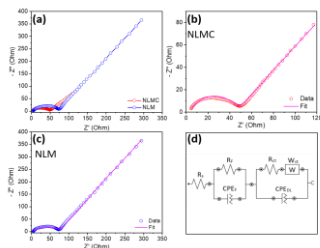


Figure 3.9. Randles–Sevcik



Hình 3.10. Nyquist plots of NLM and NLMC.

material is equivalent to or greater than most similar materials. In particular, the cycle performance of NLMC has been significantly improved, reaching 97.9 % after 100 cycles at a current density of 11 mA g^{-1} . The good electrochemical properties of NLMC material may be due to two main reasons: (1) The presence of Co in the structure of $(\text{Na,Li})\text{MnO}_2$ material leads to the simultaneous decrease of both a and c lattice constants. This phenomenon reflects the shrinkage of the crystal lattice after doping. This shrinkage helps the material structure to be more robust and stable during charging/discharging. Thereby, improving the cycle performance of the material; (2) Co directly participates in the redox reaction to create additional capacity. At the same time, Co increases the electrical conductivity of the electrode, helping the redox reaction happen easily. Therefore, it improves the specific capacity of the material.

As a result, both the specific capacity and cycle performance of the NLMC material were evaluated ($111.89 \text{ mAh.g}^{-1}$, 97.9% after 100 cycles) was significantly improved compared to the undoped NLM material (86 mAh.g^{-1} , 88.6% after 30 cycles). In addition, the charge/discharge rate of the NLMC material (63 mAh.g^{-1} at a high current density of 110 mA) was also significantly improved than NLM (17 mAh g^{-1} at high current density of 110 mA g^{-1}).

3.3. Conclusion of Chapter 3

NLM and NLMC materials were successfully synthesized by solid-state reaction method: (1) NLM material has discharge specific capacity of 86 mAh g^{-1} at current density of 11 mA g^{-1} and 17 mAh g^{-1} at 110 mA g^{-1} , cycle efficiency 88.6% (after 30 cycles at 11 mA g^{-1}); (2) NLMC material has a discharge specific capacity of $111.89 \text{ mAh g}^{-1}$ at a current density of 11 mA g^{-1} and 63 mAh g^{-1} at 110 mA g^{-1} . Cycle efficiency is about 97.9% (after 100 cycles at a current density of 11 mA g^{-1}).

CHAPTER 4. STUDY THE EFFECT OF Co, F DOPPING AND CO-DOPPING (Na,Li)MnO₂ OXIDE ON THE STRUCTURE AND ELECTROCHEMICAL PROPERTIES

4.1. The structure and morphology of the material

4.1.1. The phase structure results of the synthesized materials

The XRD pattern shows that, the structure of NLM, F-NLM, Co-NLM and CoF-NLM materials are the same. The diffraction peaks are consistent with the JCPDS standard spectrum number 27-0751, indicating

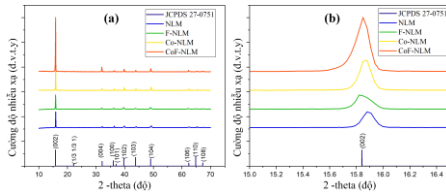


Figure 4.1. (a) X-ray diffraction pattern and (b) peak magnification region (002) of the materials.

that, these materials have a hexagonal structure, belonging to the P63/mmc space group and the magnified area of peak (002) shows the diffraction peaks slightly shifted towards the larger 2θ angle (Figure 4.1).

The lattice constants of the synthesized materials were calculated using the Rietveld fitting method. As a result, all materials showed a decrease in a constant and an increase in c constant compared to the standard material. Among them, the CoF-NLM material showed the largest decrease/increase in lattice constants.

4.1.2. Elemental composition results in the synthesized material

The energy dispersive spectra of the materials in Figure 4.2 confirm that, aside from Li which is absent due to the limit of the measurement, the elements present in the EDX spectra of the

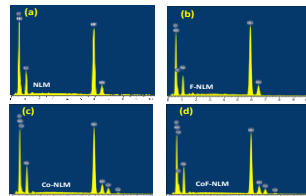


Figure 4.2. EDX results of the synthesized materials.

materials are entirely consistent with the elements present in the original precursor used. The approximate atomic ratios between Na, Li, Mn, and Co were determined using ICP-MS.

The measured results are relatively consistent with the atomic ratios in the original precursor salt mixture.

4.1.3. *The morphology of synthesized material*

The SEM image in Figure 4.3 shows that all the materials are polyhedral shape, with dimensions ranging from 3 to 5 μm , and are bonded together.

The Co, F, Co and F doped samples have secondary particles with sizes of approximately 100-500 nm on the surface of the polyhedron, making the polyhedral particle surface more prominent. The CoF-NLM sample surface has the highest level of roughness.

4.1.4. *The distribution of elements in the synthesized material*

The EDS mapping of the elements matches the TEM image of the corresponding materials (Figure 4.4). This result demonstrated that the elements Na, Mn, Co, O, and F are evenly distributed in both Co-NLM and CoF-NLM materials.

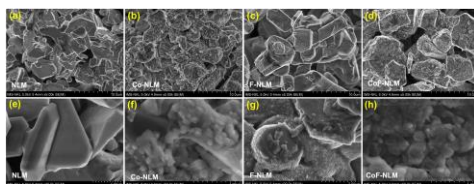


Figure 4.3. SEM images of the synthesized material at different magnifications.

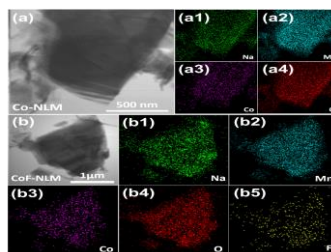


Figure 4.4. TEM images and mapping of corresponding atoms of Co-NLM and CoF-NLM.

4.1.5. The composition and redox states of the elements in the synthesized material

The XPS spectra of Mn 2p and Co 2p (Figure 4.5) confirm that the Mn^{3+}/Mn^{4+} ion ratio in CoF-NLM material (1.24) is higher than that of Co-NLM material (0.81), and the Co^{2+}/Co^{3+} ion ratio in CoF-NLM material (1.14) is higher than that in Co-NLM material (0.73).

This is because when F^- replaces O^{2-} , the crystal lattice becomes deficient in negative charge. To maintain charge neutrality, Mn^{4+} will be reduced to Mn^{3+} , and Co^{3+} will be reduced to Co^{2+} to provide the corresponding negative charge to the crystal lattice.

4.3. The electrochemical properties of synthesized materials

4.3.1. Galvanostatic Charge - Discharge results

The specific charge/discharge capacities of the second cycle of NLM, F-NLM, CoNLM, and CoF-NLM are 110.28/85.46 mAh g^{-1} , 133.73/110 mAh g^{-1} , 140.5/121.44 mAh g^{-1} , and 143.07/135 mAh g^{-1} , respectively (Figure 4.6). It can be seen that, CoF-NLM materials doped with both Co and F have better energy storage capacity compared to Co-NLM (doped with Co), F-NLM (doped with F), and undoped NLM. The specific discharge capacity of CoF-NLM materials has also been significantly

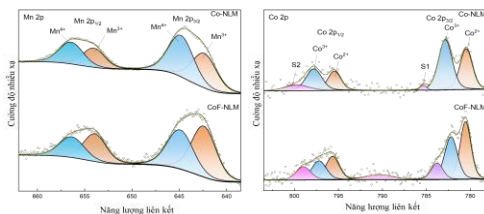


Figure 4.5. XPS survey spectra of Mn 2p and Co 2p.

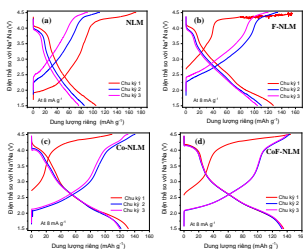


Figure 4.6. The GCD profiles of synthesized materials at 8 mA g^{-1} .

improved with some oxide materials (Na,Li)MnO₂ undoped or only cation doped in the previously published reports.

As shown in Figure 4.7, the specific capacities of all materials decrease with increasing current density. At a high current density of 100 mA g⁻¹, the NLM and F-NLM electrodes exhibit almost negligible capacities. In contrast, the CoF-NLM electrode still maintains a specific capacity of 101.15 mAh g⁻¹. This value is significantly higher than that of the Co-NLM electrode (90.25 mAh g⁻¹), indicating that the simultaneous Co and F doping effectively enhances the rate capability of the material.

Figure 4.8 is the results of 100 consecutive charge/discharge cycles at a current density of 8 mA g⁻¹. The results show that, the remaining discharge specific capacity of the Co-NLM material is 111.86 mAh g⁻¹, corresponding to 92.11% of the capacity of the second cycle. For the CoF-NLM material, the remaining discharge capacity is 126.96 mAh g⁻¹, corresponding to 94% of the capacity of the second cycle. The cycle performance value of CoF-NLM material is higher than that of Co-NLM and also higher than that of some previously published undoped or only cation doped (Na,Li)MnO₂ oxide materials.

4.3.2. Cyclic Voltammetry (CV) Analysis

On the CV curve (Figure 4.9) at a scan rate of 0.05 mV s⁻¹, there are three pairs of peaks: the redox peak, with the most pronounced peak observed at 2.5 V/2.0 V, is attributed to the redox reaction of the Mn⁺⁴/Mn⁺³ ion pair. The

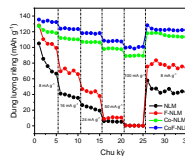


Figure 4.7. rate capacity of synthesized materials.

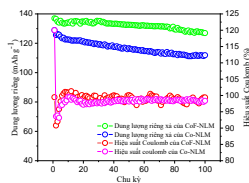


Figure 4.8. The cycling performance of Co-NLM and CoF-NLM after 100 cycles.

second, weaker peak, observed at 3.1 V/2.5 V, is attributed to the redox reaction of $\text{Co}^{+3}/\text{Co}^{+2}$. The third peak, appearing at 4.4 V/4.1 V, has not yet determined the origin. CV analysis confirms that Co directly participated in the redox reaction, increasing the material specific capacity.

4.3.3. The electrochemical impedance spectrum results

Figure 4.10 shows the Nyquist diagrams of the electrode materials before charging/discharging. The equivalent circuit diagram and the values of the elements in the circuit were determined by circuit fitting using Nova 1.11 software. As a result, the R_s and R_{ct} values of Co-NLM and CoF-NLM did not differ significantly. The resistance value of CoF-NLM was the smallest compared to the synthesized materials.

The Co-NLM and CoF-NLM materials exhibit good electrochemical properties. This can be attributed to four main factors: (1) Co doping or Co, F co-doping into the structure of $(\text{Na},\text{Li})\text{MnO}_2$ material synthesized by the sol-gel method reduces the a constant and increases the c lattice constant. The decrease in a constant makes the MO_2 framework more stable, thereby improving the cycle performance of the material. The increase in c lattice constant reflects the widening of the distance between the metal oxide layers of MO_2 , allowing Na^+ ions to easily insert into/exit and diffuse in the material, thereby improving the capacity and kinetics of the electrochemical reaction occurring in the material; (2) The morphology of the materials shows that Co-NLM and CoF-NLM materials

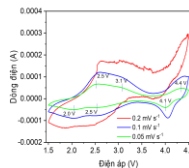


Figure 4.9. CV curves of CoF-NLM at difference scan rates.

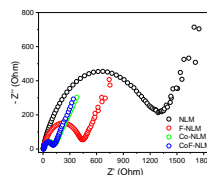


Figure 4.10. Nyquist plots of synthesized materials.

have a rougher surface, allowing the electrode to better contact the electrolyte, thereby improving the electrochemical properties of the material; (3) Co can directly participate in redox reactions and improve the electrical conductivity of the electrode, thereby promoting the kinetics of the electrochemical process and contributing to the improvement of the specific capacity of the material. (4) The presence of F increases the $\text{Mn}^{3+}/\text{Mn}^{4+}$ and $\text{Co}^{2+}/\text{Co}^{3+}$ ratios, which means increasing the active transition metal for electrochemical reactions leading to improved specific capacity.

4.4. Conclusion of Chapter 4

Co-NLM and CoF-NLM materials were successfully fabricated using the sol-gel method: (1) Co-NLM material had a specific capacity of $121.44 \text{ mAh g}^{-1}$ at a current density of 8 mA g^{-1} and 90.25 mAh g^{-1} at 100 mA g^{-1} , the cycle efficiency of the material was approximately 92.11% after 100 cycles at a current density of 8 mA g^{-1} . (2) CoF-NLM material had a specific capacity of 135 mAh g^{-1} at a current density of 8 mA g^{-1} and $101.15 \text{ mAh g}^{-1}$ at a high current density of 100 mA g^{-1} , with a cycle efficiency of approximately 94% after 100 cycles at a current density of 8 mA g^{-1} .

OVERALL CONCLUSION

The dissertation "Synthesis and investigation of the electrochemical characteristics of Co, F doped and co-doped (Na,Li) MnO_2 oxide as cathode for sodium-ion batteries" was conducted at the Academy of Science and Technology and the Institute of Materials Science, Vietnam Academy of Science and Technology. The dissertation focused on the fabrication of several Co, F doped and co-doped (Na,Li) MnO_2 oxide materials. Simultaneously, investigating the structure, morphology, and electrochemical properties of the synthesized materials to clarify the influence of each doping element on the structure and electrochemical properties of the synthesized materials. The results

of the dissertation have been published in prestigious journals, including: 2 articles in SCIE-listed journals and 2 articles in national journals.

The dissertation has achieved the objectives set, specifically:

1. Successfully synthesized materials that can be applied as positive electrodes for SIBs based on the Co, F doped and Co-doped (Na,Li)MnO₂ oxide system using different methods. All synthesized materials have a hexagonal structure, belong to the P63/mmc space group, and have particle sizes in the range of 1-5 μm, including:

- Na_{0.67}Li_{0.33}Mn_{0.95}Co_{0.05}O₂ (NLMC) material, synthesized by solid-state reaction, providing a discharge specific capacity of 111.89 mAh.g⁻¹ at a current density of 11 mA g⁻¹ and 63 mAh g⁻¹ at a high current density of 110 mA g⁻¹, with a cycle efficiency of 97.9% (after 100 cycles at a current density of 11 mA g⁻¹).

- The Na_{0.8}Li_{0.1}Mn_{0.8}Co_{0.1}O₂ (Co-NLM) material, synthesized by sol-gel method, provided a discharge specific capacity of 121.44 mAh g⁻¹ at 8 mA g⁻¹ and 90.25 mAh g⁻¹ at 100 mA g⁻¹, with a cycle efficiency of 92.11% (after 100 cycles at 8 mA g⁻¹);

- The Na_{0.8}Li_{0.1}Mn_{0.8}Co_{0.1}F_{0.1}O₂ (CoF-NLM) material, synthesized by sol-gel method, provided a discharge specific capacity of 135 mAh g⁻¹ at a current density of 8 mA g⁻¹ and 101.15 mAh g⁻¹ at a high current density of 100 mA g⁻¹, with a cycle efficiency of 94% (after 100 cycles at a current density of 8 mA g⁻¹).

2. The influence of doping elements and synthesis methods on the structure and electrochemical properties of the material has been clarified, specifically:

- Co doping by solid-state reaction reduces both a and c lattice constants simultaneously. While Co doping and Co, F co-doping by sol-gel method reduces a lattice constant and increases c lattice constant. This

structural change has contributed to improving the electrochemical properties of the material.

• Ions doping can directly affect the energy storage process: (1) Co^{2+} can directly participate in redox reactions, increasing the specific capacity of the material. On the other hand, Co also increases the electrical conductivity of the electrode, helping to improve the kinetics of the electrochemical reaction occurring on the electrode; (2) F increases the active transition metal ions, that mean: increases the number of electrochemical active sites, thereby improving the specific capacity of the material.

3. The research results of this dissertation have contributed to clarifying the relationship between composition doping – crystal structure – electrochemical properties of cathode materials based on the $(\text{Na,Li})\text{MnO}_2$ material system. These results provide more knowledge for the design and optimization of high-electrochemical materials used as cathodes for SIBs, and open up research directions for developing low-cost, environmentally friendly cathode materials suitable for research and production conditions in Vietnam.

FUTURE RESEARCH DIRECTIONS

1. Continue research and optimize the Li/Co/F ratio to create materials with even better electrochemical properties, contributing to the development of positive electrode material systems for SIBs.

2. Utilize advanced techniques such as XPS and in-situ TEM to directly monitor the structural and valence changes of transition metals during charging/discharging, thereby gaining a better understanding of the electrochemical mechanism of the materials.

LIST OF PUBLICATIONS RELATED TO THE THESIS

1. **Nguyen Thi Thu Hoa**, Nguyen Van Ky, Luong Trung Son, Dinh Tien Dung, To Van Nguyen, Vu Dinh Lam, Nguyen Van Nghia, “*Facile synthesis of cobalt - doped sodium lithium manganese oxide with superior rate capability and excellent cycling performance for sodium - ion battery*”, Journal of Electroanalytical Chemistry, 929, p. 117129 (2023).

2. **Thu Hoa Nguyen Thi**, Nguyen To Van, Minh Triet Dang, Nguyen Vo Anh Duy, Trung Son Luong, Son Dinh Le, Tuan Nguyen Van, Dinh Lam Vu, Nghia Nguyen Van, “*Co and F co-doping to augmenting the electrochemical performance of P2-type sodium lithium manganese oxide for sodium ion battery*”, Journal of Electroanalytical Chemistry, 972, p. 118590 (2024).

3. **Nguyen Thi Thu Hoa**, Nguyen Van Nghia, Nguyen Van Ky, Ngo Quy Quyen, Vu Dinh Thao, Le Van Toan, Vu Dinh Lam, “*synthesis and electrochemical characteristics of zinc-doped sodium manganese oxide as a cathode material for sodium-ion batteries*”, Le Qui Don Technical University: Journal of Science and Technique, 1(01),p. 30, (2023).

4. Nguyen Van Nghia, Nguyen Van Ky, Vu Dinh Lam, **Nguyen Thi Thu Hoa***, “*synthesis and characterization of P2-Na_{1.0}Li_{0.15}Mn_{0.8}Ni_{0.2}O₂ material for cathode in sodium-ion batteries*”, TNU Journal of Science and Technology, 230(14), p. 369, (2025).